Time-resolved X-ray diffraction at NERL

KENICHI KINOSHITA, HIDEKI HARANO,* KOJI YOSHII, TAKERU OHKUBO,
ATSUSHI FUKASAWA, KEI NAKAMURA, AND MITSURU UESAKA

Nuclear Engineering Research Laboratory, University of Tokyo, 2-22 Shirane Shirakata, Tokai, Naka, Ibaraki 319-1188, Japan

(RECEIVED 30 November 2000; ACCEPTED 5 February 2001)

Abstract

For ultrafast material analyses, we constructed the time-resolved X-ray diffraction system utilizing ultrashort X-rays from laser-produced plasma generated by the 12-TW–50-fs laser at the Nuclear Engineering Research Laboratory. Ultrafast transient changes in laser-irradiated GaAs crystals were observed as X-ray diffraction patterns. Experimental results were compared with numerical analyses.

1. INTRODUCTION

New remarkable possibilities have been introduced to the time-resolved material analyses by development on laboratory-scale sources of ultrashort X-ray pulses which have been made accessible by progress in ultraintense and ultrashort laser technologies such as a table-top terawatt laser. Nowadays laser intensity of 10^{16} to 10^{18} W/cm^2 is achievable by focusing a high power laser to a small spot. Such intense laser pulses can easily generate hot plasmas by interacting with solid targets, making energetic electrons which produce X rays by hitting the solid. These X rays can have short pulse durations because of the short interaction time between the laser and the plasmas, and the rapid cooling of the plasmas. Therefore we can utilize these X rays as probes to investigate ultrafast phenomena in materials within the method called time-resolved X-ray diffraction. Up until now, this method has usually been used in combination with synchrotron radiations with the time resolution longer than picosecond (Larson *et al.*, 1986; Kojima *et al.*, 1995; Larsson *et al.*, 1998). Recently pico- to subpicosecond X-ray pulses were produced by Thomson scattering of ultrashort laser pulses synchronized to relativistic electron beams (Esarey *et al.*, 1993; Kim *et al.*, 1994; Schoenlein *et al.*, 1996; Leemans *et al.*, 1997). It was shown that laser-produced plasma X-rays would also generate such short pulses as several picoseconds (Yoshida *et al.*, 1998) and subpicoseconds in appropriate conditions (Reich *et al.*, 2000). Those X rays,

having been applied to the dynamic analysis of materials (Rischel *et al.*, 1997; Chin *et al.*, 1998; Rose-Petruck *et al.*, 1999), are expected to provide the promising tool for investigation of ultrafast unknown phenomena and experimental verification of solid-state physics.

At the Nuclear Engineering Research Laboratory (NERL), University of Tokyo, we have been studying ultrafast phenomena such as pulse radiolysis, laser–plasma interaction, and wake-field acceleration, using the femtosecond laser system and subpicosecond electron linacs. Several experiments have been also carried out at NERL such as Thomson scattering X-ray generation by colliding subpicosecond electron pulses with terawatt laser pulses (Kotaki *et al.*, 1999) and characteristic X-ray generation by hitting solid targets with energetic electron beams (Harano *et al.*, 2000) to generate ultrashort X-ray pulses to be applied to the time-resolved analysis.

Recently we installed the 12-TW–50-fs laser system for further investigations of ultrashort pulse generation, time-resolved analysis, and so on. Here in this paper, we demonstrate the time-resolved X-ray diffraction applied to the transient strain propagation in gallium arsenide induced by the ultrashort laser irradiation utilizing the ultrashort X-ray pulses generated using the 12-TW–50-fs laser system.

2. EXPERIMENTS

Figure 1 shows the experimental setup for the time-resolved X-ray diffraction. The laser pulse coming into the vacuum chamber is divided into the main pulse and the pump pulse in a ratio of nine to one by the beam splitter. The former is focused onto the copper target with the off-axis parabolic mirror (focal length = 162 mm) to generate the laser-

---

Address correspondence and reprint requests to: Kenichi Kinoshita, Nuclear Engineering Research Laboratory, University of Tokyo, 2-22 Shirane Shirakata, Tokai-mura, Naka-gun, Ibaraki 319–1188, Japan. E-mail: kino@tokai.t.u-tokyo.ac.jp

*Current address: O-arai Engineering Center, Japan Nuclear Cycle Development Institute, 4002 Narita, O-arai, Ibaraki 311-1393, Japan.
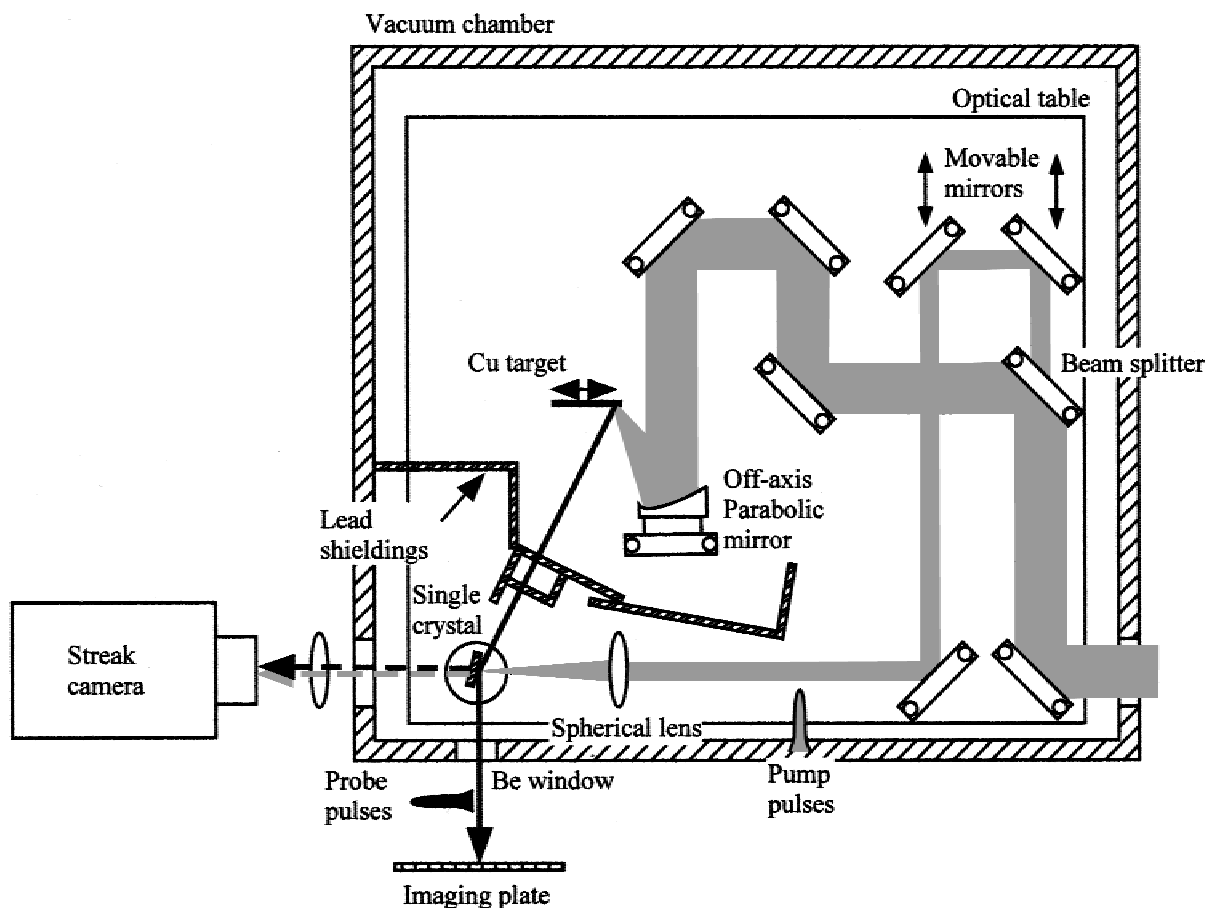
Fig. 1.

produced plasma X rays that are used for X-ray diffraction from the single crystal as the probe pulse. Focused by the spherical lens, the latter induces transient phenomena inside the crystal after passing through the delay path with which the time interval between the pump and probe pulses can be controlled. For easy alignment, large wafers or disks of single crystals are employed as the samples for X-ray diffraction and mounted on the automatic positioner. The two-dimensional diffraction images are taken by X-ray imaging plates (BAS-SR, Fuji Photo Film) with the spatial resolution of 50 μm. The samples are surrounded by lead plates for shielding of the background X rays scattered from the circumference. The X rays may reach the sample surface only through the 3-mm-wide slit. Polyvinylidene chloride film is put in front of the parabolic mirror as a protection against ablated debris from the copper target. Diffracted X-rays pass through the beryllium window and are measured by the imaging plates outside of the chamber. Another 1-cm-wide slit is put at the exit of the beryllium window to reduce the background X rays.

To determine the zero point of delay time where the pump pulse and the probe pulse reach the crystal surface at the same time, we used the femtosecond streak camera. A mir-

ror with a hole at the center is placed instead of the crystal in Figure 1 with a proper angle to guide the light from the focal point of the parabolic mirror reflected and scattered by the copper target toward the streak camera. This light from the copper target substitutes for the X-ray pulse while the pump pulse can directly reach the streak camera by passing through the hole of the mirror. Figure 2 shows an image of the streak camera and its temporal profile. The pump pulse comes 7.2 ps prior to the light from the copper in Figure 2. We can adjust the distance between the pump pulse and the probe pulse to be zero by changing the delay path. The pulse width of the pump pulse appears to be 0.55 ps in this measurement, which agrees with the time resolution of the streak camera, about 0.5 ps, in this range. On the other hand, measured width of the light from the copper target is 0.73 ps and it differs from the time resolution. There can be some reasons of this elongation such as, for example, the size of the light source due to bad focusing or dispersion of the optics. In any case, we can still determine the zero point with precision of about 1 ps in principle.

X-ray diffraction experiments were carried out with the configuration shown in Figure 1. Figure 3 shows a diffraction image taken by the imaging plate and its horizontal
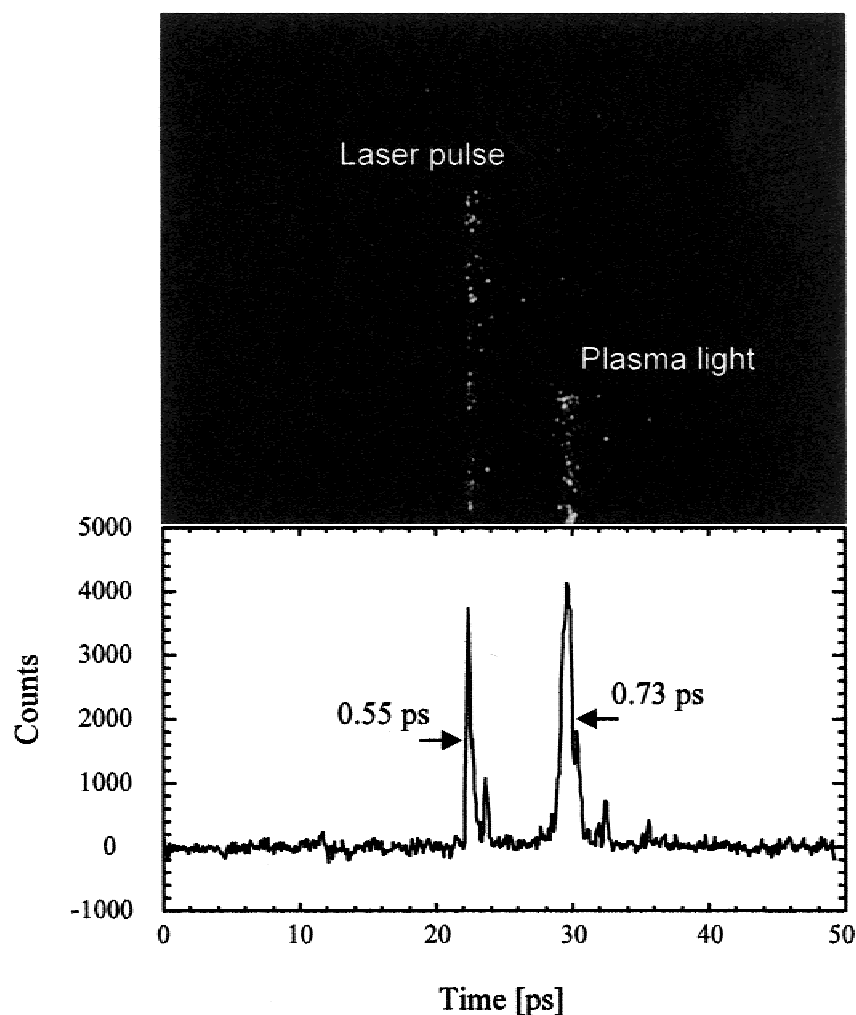
Fig. 2.

profile of X-ray intensity from a GaAs wafer of (111) orientation with pump pulses of 1.3 mJ/mm^2 with 150-ps delay. The accumulation time of this image was about 30 s at 10 Hz repetition. The two thick lines in Figure 3 are composed of characteristic X-rays from the copper, that is, CuKα1(1.5407 Å) and CuKα2(1.5439 Å). The left-hand side of the image corresponds to the smaller angle of diffraction and the right-hand side to the larger. The lattice distance of GaAs(111) is 3.254 Å and this makes the diffraction angles for CuKα1 and CuKα2 13.65° and 13.68°, respectively. We can see an extra line on the left of the original lines in the image at the laser-irradiated region. This line is caused by deformation of the lattice of the GaAs crystal induced by the laser pulses, resulting in a subpeak in the profile.

Figure 4 shows the temporal evolution of diffraction profiles. Negative delay in Figure 4 means that the probe pulse comes prior to the pump pulse. Naturally, we can see only two peaks composed of Kα1 and Kα2 at −50 ps from the undisturbed crystal and there is no change at 0 ps. A small subpeak can be seen on the left of Kα1 at 50 ps. At 100 ps, the subpeak is small but narrow while Kα2 is blurred. The

position of the subpeak becomes closer to the peak of Kα1 as delay time increases during 150 ps to 250 ps and it merges into Kα1 at 300 ps.

These changes of the diffraction profiles in Figure 4 are directly brought about from ultrafast evolution of the lattice in the crystal in a picosecond time scale. The laser coming into the crystal will excite electrons in the valence band to the conduction band and thus undertake absorption by making electron-hole pairs. Therefore energy deposit will be distributed according to this absorption length. Then energy transfer from carriers to lattice will occur by scattering. This brings a rapid temperature increase in the crystal, resulting in thermal stress in the lattice. This thermal stress triggers a strain wave propagating into the crystal with the speed of sound. The time-resolved X-ray diffraction can pick out snapshots of the crystal undergoing the above process.

3. NUMERICAL ANALYSIS

We also performed calculations of X-ray diffraction from laser-irradiated crystal. Laser-induced strain derived by
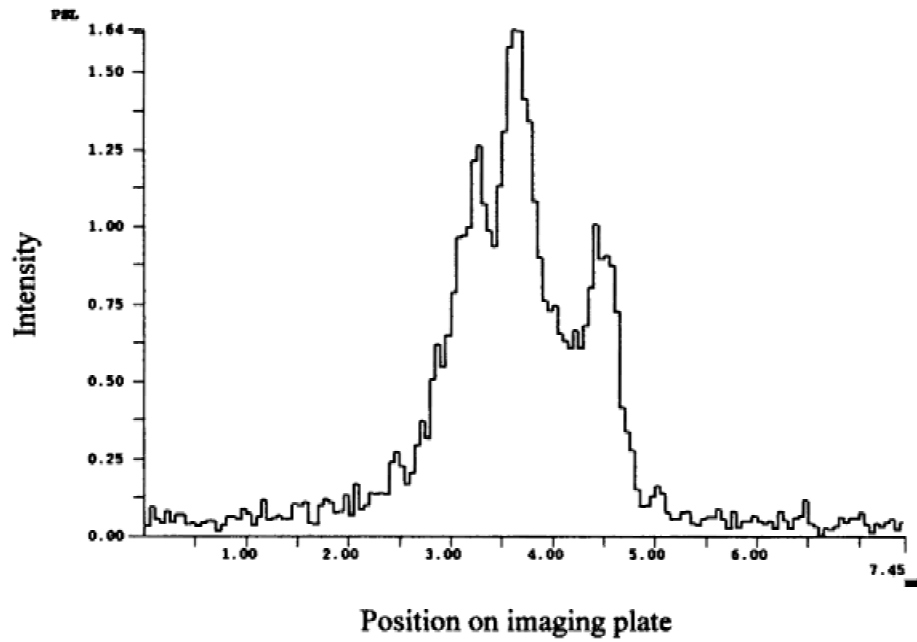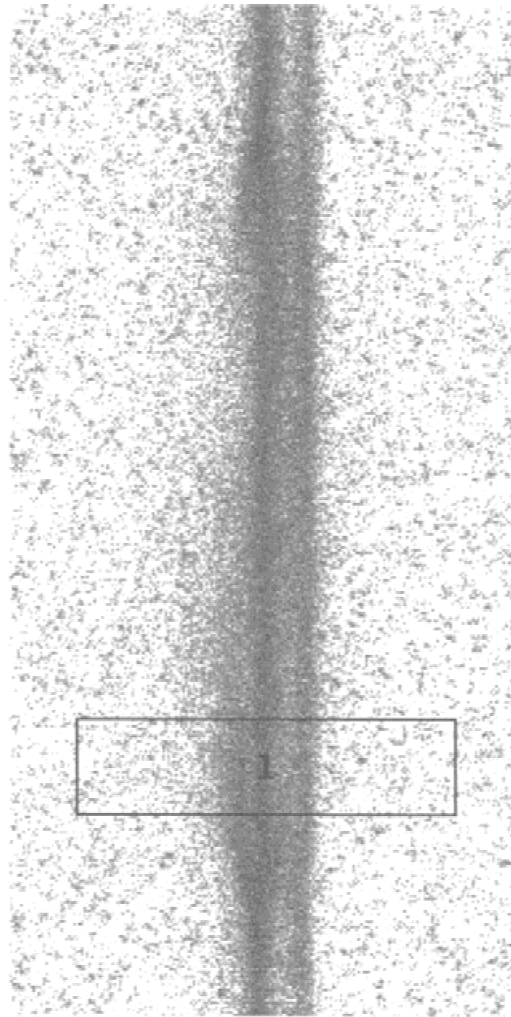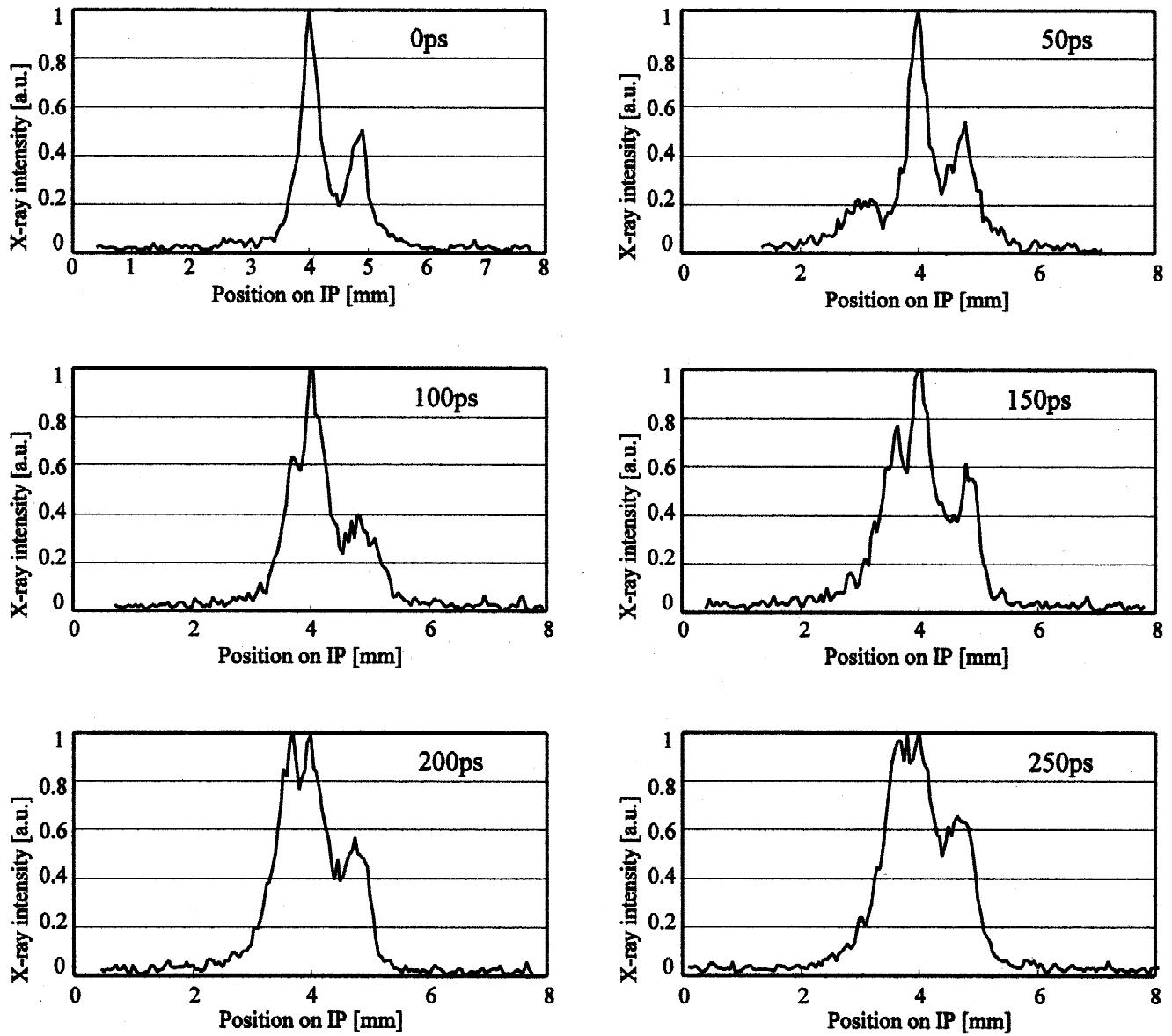
Fig. 3.

Fig. 4.

Thomsen *et al.* (1986) was assumed and temporal evolution of X-ray diffraction patterns was calculated. The laser energy absorbed in the crystal makes the temperature increase distributed according to the absorption length ζ (Blakemore, 1982). Thus, the temperature increase ΔT can be described as

$$\Delta T(z) = \Delta T_s \, e^{z/\zeta}, \tag{1}$$

where z is the distance from the surface into the crystal and ΔT_s is the temperature increase at the surface just after the laser irradiation. This temperature distribution gives rise to a thermal stress given by

$$-3B\beta\Delta T(z), \tag{2}$$

where B is the bulk modulus and β is the linear expansion coefficient. Then thermal elastic equations are given by

$$\sigma_{33} = 3\,\frac{1-\nu}{1+\nu}\,B\eta_{33} - 3B\beta\Delta T(z), \tag{3}$$

$$\rho\,\frac{\partial^2 u_3}{\partial t^2} = \frac{\partial \sigma_{33}}{\partial z}, \tag{4}$$

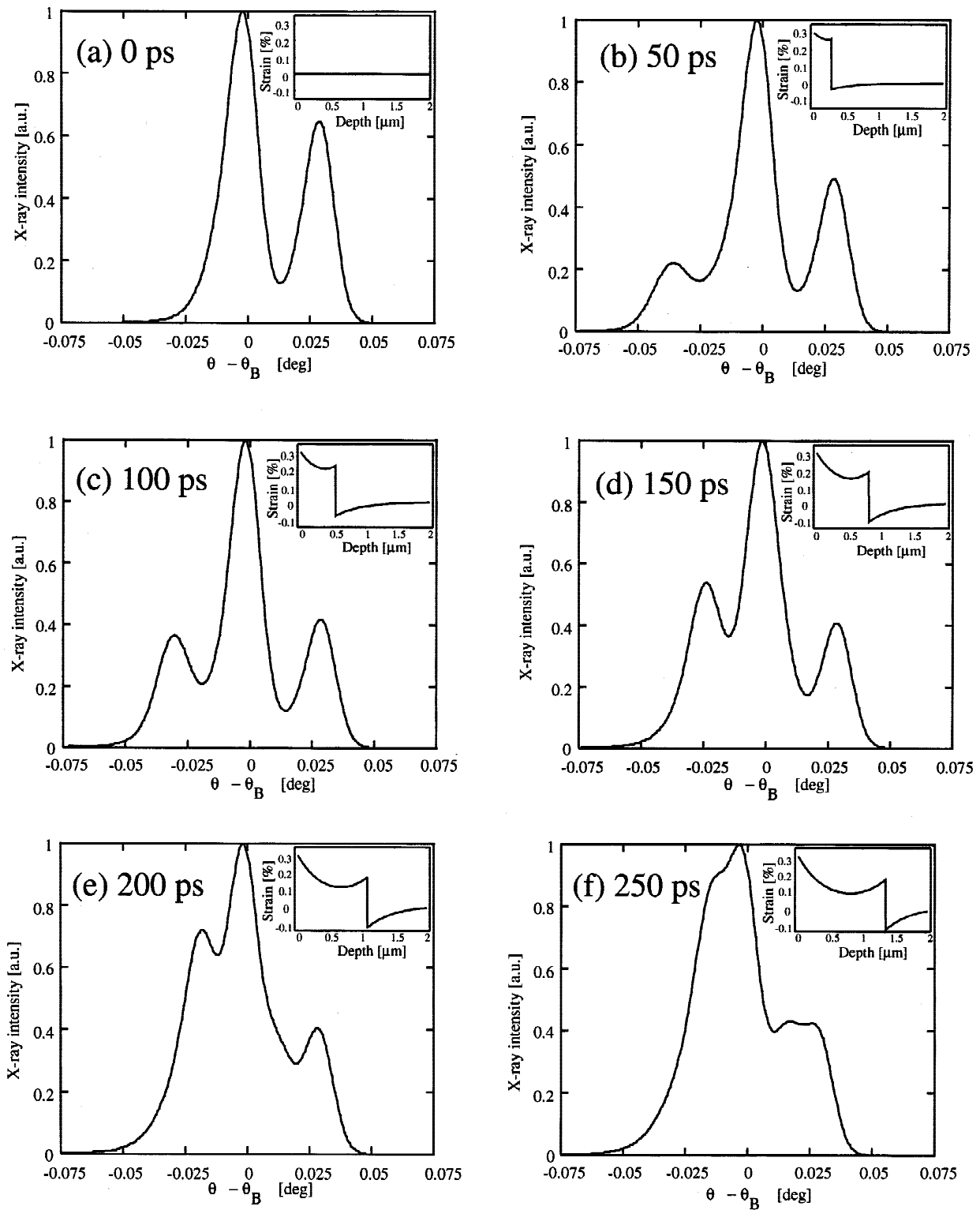$$\eta_{33} = \frac{\partial u_3}{\partial z}, \tag{5}$$

Fig. 5.

where η_{33} is the elastic strain tensor, ν is Poisson's ratio, u_3 is the displacement in the z direction, and ρ is the density. The initial condition is that $\sigma(z) = 0$ everywhere. These equations can be solved analytically. The solution is

$$\eta_{33}(z,t) = \Delta T_s \frac{1+\nu}{1-\nu} \left[e^{-z/\zeta} \left(1 - \frac{1}{2} e^{vt/\zeta} \right) \right.$$

$$\left. - \frac{1}{2} e^{-|z-vt|/\zeta} \operatorname{sgn}(z-vt) \right], \qquad (6)$$

where v is the sound velocity. This solution gives two components, that is, a strain wave propagating inward with the speed of sound and a thermal expansion of the lattice at the surface. X-ray diffraction patterns were calculated with this strain based on the kinetic diffraction theory. Figure 5 shows calculated results with corresponding crystal strains (inset). An additional peak arises at a smaller diffraction angle due to the X-ray diffraction of Kα1 from the expanded lattice, and it gets closer to the original angle as the strain wave goes more inside as shown in Figure 5b–f.

4. CONCLUSION

We constructed the time-resolved X-ray diffraction system utilizing the laser-produced plasma X-ray generated with the 12-TW–50-fs laser at the Nuclear Engineering Research Laboratory, University of Tokyo. The system was applied to the dynamic analysis for the laser-irradiated GaAs(111). Picosecond temporal evolution of X-ray diffraction was demonstrated. We also performed the calculation of X-ray diffraction from the laser-irradiated crystal. We plan to apply this technique to the dynamic analysis of other materials such as metals, ferroelectrics, and organic substances.

REFERENCES

BLAKEMORE, J.S. (1982). *J. Appl. Phys.* **53**, R123.

CHIN, A.H., SCHOENLEIN, R.W., GLOVER, T.E., HEIMANN, P., LEEMANS, W.P., SHANK, C.V., ZOLOTOREV, M.S. & ZHOLENTS, A.A. (1998). *Conf. Proc. Int. LEOS Annu. Meet.* **11**, 134.

ESAREY, E., SPRANGLE, P., TING, A. & RIDE, S.K. (1993). *Nucl. Instrum. Meth. A* **331**, 545.

HARANO, H., KINOSHITA, K., YOSHII, K., UEDA, T., OKITA, S. & UESAKA, M. (2000). *J. Nucl. Matr.* **280**, 255.

KIM, K.-J., CHATTOPADHYAY, S. & SHANK, C.V. (1994). *Nucl. Instrum. Meth. A* **341**, 351.

KOJIMA, S., KUDO, Y., KAWADO, S., ISHIKAWA, T. & MATSU-SHITA, T. (1995). *Rev. Sci. Instrum.* **66**, 1419.

KOTAKI, K., NAKAJIMA, K., KANDO, M., DEWA, H., KONDO, S., SAKAI, F., WATANABE, T., UEDA, T., NAKANISHI, H., YOSHII, K., OGATA, A., KINOSHITA, K. & UESAKA, M. (1999). *Proc. Sixth International Conference on X-ray Lasers*, Kyoto, Japan, 31 August–4 September 1998, Inst. Phys. Conf. Ser. No. 159 (IOP, Bristol) p. 565.

LARSON, B.C., TISCHLER, J.Z. & MILLS, D. (1986). *J. Mater. Res.* **1**, 144.

LARSSON, J., LINDENBERG, A.M., SCHUNK, P.J., FALCONE, R.W., HEIMANN, P.A., PADMORE, H.A., BUCKSBAUM, P.H., LEE, R.W. & WARK, J.S. (1998). *Appl. Phys. A* **66**, 587.

LEEMANS, W.P., SCHOENLEIN, R.W., VOLFBEYN, P., CHIN, A.H., GLOVER, T.E., BALLING, P., ZOLOTOREV, M., KIM, K.-J., CHATTOPADHYAY, S. & SHANK, C.V. (1997). *IEEE J. Quantum Electron.* **33**, 1925.

REICH, C., GIBBON, P., USCHMANN, I. & FÖRSTER, E. (2000). *Phys. Rev. Lett.* **84**, 4846.

RISCHEL, C., ROUSSE, A., USCHMANN, I., ALBOUY, P.-A., GEINDRE, J.-P., AUDEBERT, P., GAUTHIER, J.-C., FÖRSTER, E., MARTIN, J.-L. & ANTONETTI, A. (1997). *Nature* **390**, 490.

ROSE-PETRUCK, C., JIMENEZ, R., GUO, T., CAVALLERI, A., SIDERS, C.W., RÁKSI, F., SQUIER, J.A., WALKER, B.C., WILSON, K.R. & BARTY, C.P. (1999). *Nature* **398**, 310.

SCHOENLEIN, R.W., LEEMANS, W.P., CHIN, A.H., VOLFBEYN, P., GLOVER, T.E., BALLING, P., ZOLOTOREV, M., KIM, K.-J., CHATTOPADHYAY, S. & SHANK, C.V. (1996). *Science* **274**, 236.

THOMSEN, C., GRAHN, H.T., MARIS, H.J. & TAUC, J. (1986). *Phys. Rev. B* **34**, 4129.

YOSHIDA, M., FUJIMOTO, Y., HIRONAKA, Y., NAKAMURA, K.G., KONDO, K., OHTANI, M. & TSUNEMI, H. (1998). *Appl. Phys. Lett.* **73**, 1.